Supporting information for the article:

Understanding the solar-driven reduction of CO_2 on doped ceria

Enrique V. Ramos-Fernandez*, N. Raveendran Shiju*, Gadi Rothenberg

E-mail e.v.ramosfernandez@uva.nl or n.r.shiju@uva.nl

Van 't Hoff Institute for Molecular Sciences, University of Amsterdam, P.O. Box 94157, 1090GD Amsterdam, The Netherlands.

Kinetic Models

Kinetics models for reactions at surfaces are the subject of much research. Khawam and Flanagan give an excellent comprehensive overview of the various models.[1] Here we follow their notation for those models that are relevant to the redox cycling discussed in the main manuscript. Based on mechanistic assumptions, models are divided into nucleation, geometrical contraction, diffusion, or reaction-order (see Table S1).

Nucleation: Crystals have fluctuating local energies from imperfections due to impurities, surfaces, edges, dislocations, cracks, and point defects. Such imperfections are sites for reaction nucleation since the reaction activation energy is minimized at these points. Thus, they are called, nucleation sites. The nucleation models included on the table are derived based on two assumptions; nucleation is single- or multistepped.

Geometrical Contraction (R) Models. These models assume that nucleation occurs rapidly on the surface of the crystal. The rate of degradation is controlled by the resulting reaction interface progress toward the center of the crystal. Depending on crystal shape, different mathematical models may be derived.

Diffusion (D) Models. This model assumes the formation of a product layer around the solid, which affects the mobility of constituents. The thickness of the layer may increase depending on the reaction progress. In diffusion-controlled reactions, the rate of product formation decreases proportionally with the thickness of the product barrier layer. For metallic oxidation, this involves a moving boundary and is considered a "tarnishing reaction". Different models can be derived from different solid geometries.

Order-Based (F) Models. This model assumes that the reaction rate is proportional to concentration, amount or fraction remaining of reactant(s) raised to a particular power (integral or fractional) which is the reaction order. Since these types of models are similar to those used in homogeneous kinetics, they are the simplest models.

Table S1. Differential and integral expressions for the various models used in this study.[a,b)]

Model	Differential form $f(\alpha)=\frac{1}{k}\frac{d\alpha}{dt}$	Integral form $g(\alpha)=kt$
Nucleation models		
Power low (P2)	$2\alpha^{\frac{1}{2}}$	$\alpha^{\frac{1}{2}}$
Power low (P3)	$3\alpha^{\frac{2}{3}}$	$\alpha^{\frac{1}{3}}$
Power low (P4)	$4\alpha^{\frac{3}{4}}$	$\alpha^{\frac{1}{3}}$
Avrami-Erofeyev (A2)	$2(1-\alpha)\left[-\ln(1-\alpha)\right]^{\frac{1}{2}}$	$\left[-\ln(1-\alpha)\right]^{\frac{1}{2}}$
Avrami-Erofeyev (A3)	$3(1-\alpha)\left[-\ln(1-\alpha)\right]^{\frac{2}{3}}$	$\left[-\ln(1-\alpha)\right]^{\frac{1}{3}}$
Avrami-Erofeyev (A4)	$4(1-\alpha)\left[-\ln(1-\alpha)\right]^{\frac{3}{4}}$	$\left[-\ln(1-\alpha)\right]^{\frac{1}{4}}$
Prout-Tompkins (B1)	$\alpha(1-\alpha)$	$\ln\left[\frac{\alpha}{1-\alpha}\right]+e^{\alpha}$
Geometrical contraction models		
Contracting area (R2)	$2(1-\alpha)^{\frac{1}{2}}$	$1-(1-\alpha)^{\frac{1}{2}}$
Contracting area (R3)	$3(1-\alpha)^{\frac{1}{3}}$	$1-(1-\alpha)^{\frac{1}{3}}$
Diffusion models		
1-D diffusion (D1)	$2(1-\alpha)\left[-\ln(1-\alpha)\right]^{\frac{1}{2}}$	α^2
2-D diffusion (D2)	$-\left[\frac{1}{\ln(1-\alpha)}\right]$	$\left((1-\alpha)\ln(1-\alpha)\right)+\alpha$
3-D diffusion Jander (D3)	$\left[\frac{3(1-\alpha)^{\frac{2}{3}}}{2\left(1-(1-\alpha)^{\frac{1}{3}}\right)}\right]$	$\left[1-(1-\alpha)^{\frac{1}{3}}\right]^2$
Ginstling-Brounshtein (D4)	$\frac{3}{\left[2\left((1-\alpha)^{-\frac{1}{3}}\right)-1\right]}$	$1-\left(\frac{2}{3}\right)\alpha-(1-\alpha)^{\frac{2}{3}}$
Reaction order models		
Zero order (F0/R1)	1	α
First order (F1)	$1-\alpha$	$-\ln(1-\alpha)$
Second order (F2)	$(1-\alpha)^2$	$\left[\frac{1}{1-\alpha}\right]-1$
Third order (F3)	$(1-\alpha)^3$	$\frac{1}{2}\left[(1-\alpha)^{-2}-1\right]$

[a)] Adapted for the detail review about solid state kinetics reported by Khawam and Flanagan.[1]

[b)] In this table, α is the conversion, $f(\alpha)$ is the differential form of the kinetic model, and $g(\alpha)$ is the integral form of the model.

X-ray diffraction

Figure S1 shows the XRD patterns of several doped materials before and after the redox cycling. It shows the fingerprint pattern of fluorite structure, both before and after being used. The main difference between the used and fresh materials is the crystallinity. Used materials show sharpest peaks indicating the large crystals. This indicates sintering during the redox cycling.

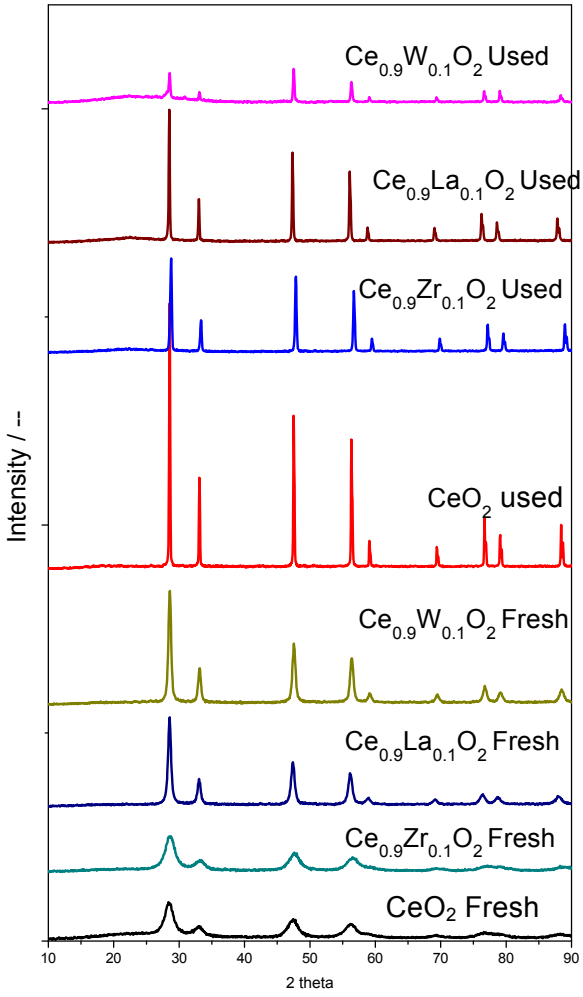

Figure S1. XRD patterns of fresh and used ceria and doped ceria samples.

Nitrogen adsorption isotherms.

Figure S2 shows the N_2 adsorption isotherms of the both pure ceria (CeO_2) and $Ce_{0.9}Zr_{0.1}O_2$. The surface area decreases after the redox treatment indicating the formation of a nonporous solid.

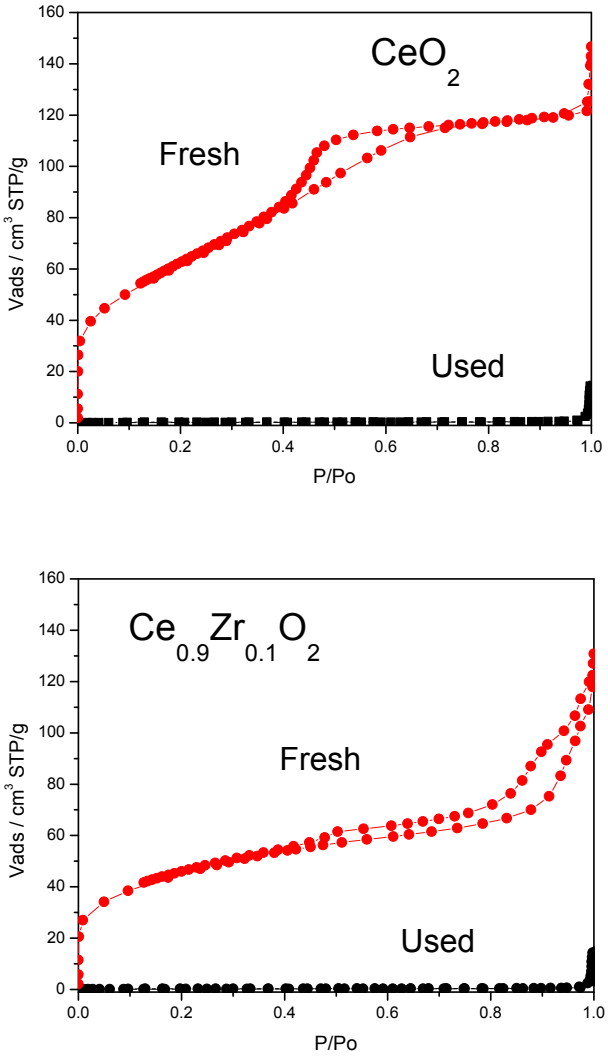

Figure S2. N_2 adsorption isotherms of fresh and used ceria and doped ceria samples.

Redox cycles for all the doped cerias.

Figure S3 presents a typical redox cycle for the pure ceria sample. From the black line one can calculate the amount of Ce(III) produced as well as the re-oxidation degree of the Ce(III) when CO_2 is fed. From the difference between the top and bottom part of the black line, we can calculate how much CO is produced in every cycle. We have done these type of experiments for 9 different materials. In all the cases, we did not detect a loss of CO production within the first 5 cycles. We then averaged the CO production for the first 5 cycles, and we take this value as CO capacity for every material. Figure S4 shows these values for $Ce_{0.9}M_{0.1}O_2$ (M= Zr, Y, V, Cr, W, Ti, La).

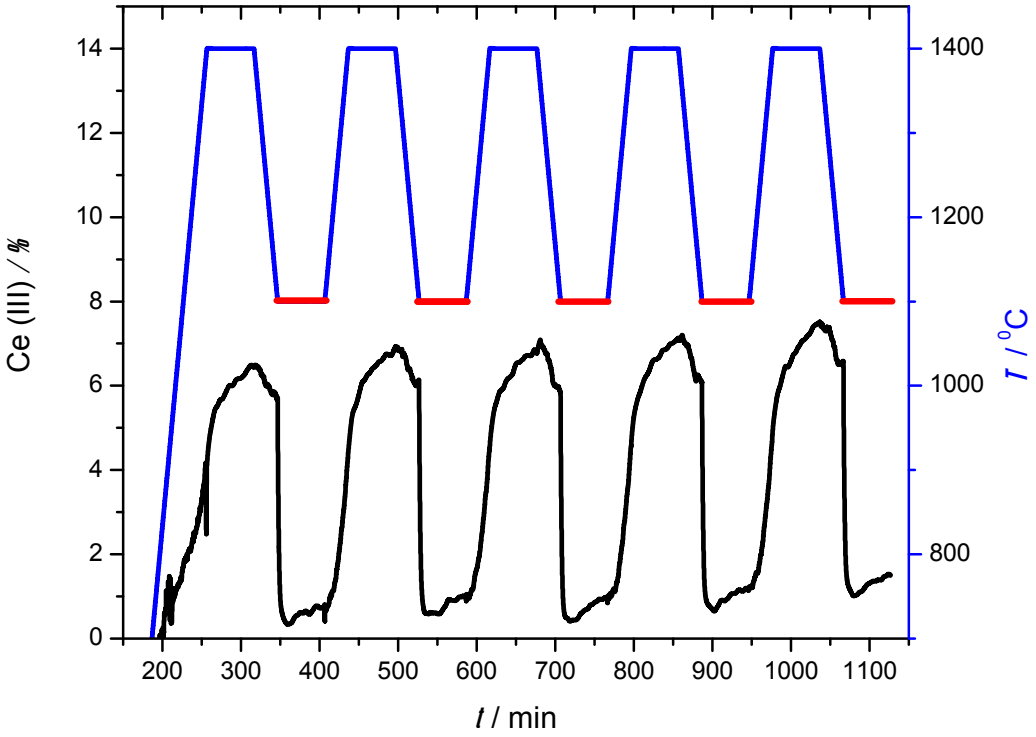

Figure S3. The graphs shows the redox cycling at isothermal conditions, oxidation (1100 °C) and reduction (1400 °C) for the pure ceria sample. The blue stepped line shows the temperature program, while the black lines show the Ce(III) concentration. Red line gives the steps where CO_2 is fed.

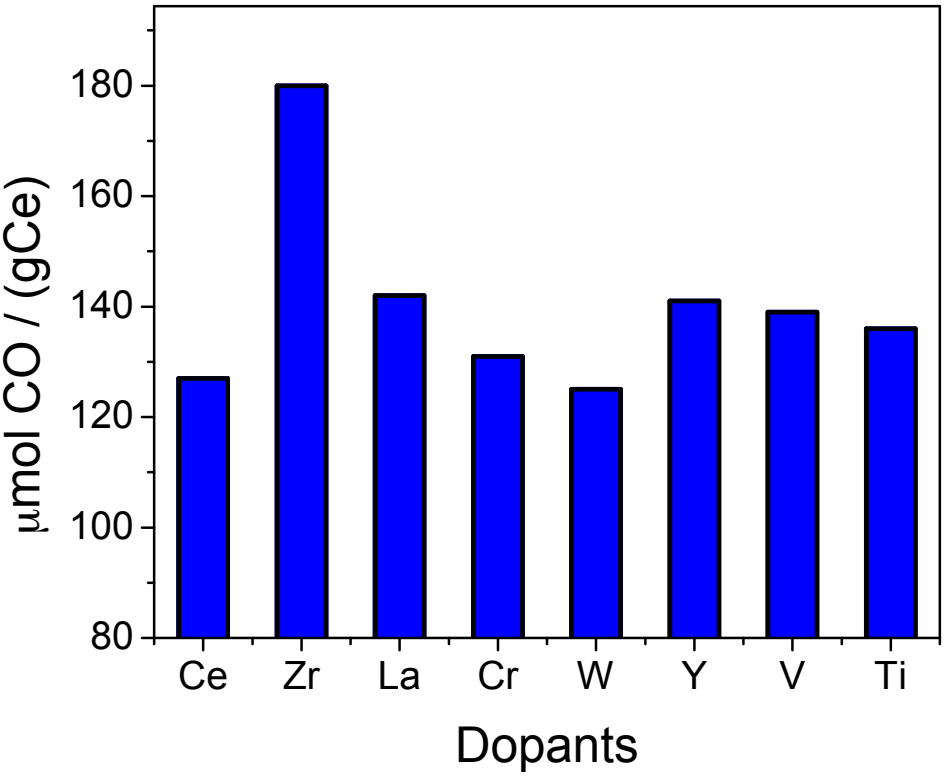

Figure S4. CO production for 8 different ceria doped materials. The concentration of dopant was 10 wt.% for all the samples

1. Khawam, A.; Flanagan, D. R., *J Phys Chem B* **2006,** *110* (35), 17315-17328.